Iranian Journal of Geophysics, Vol 15 No 4, 2022, Page 89 – 100 (Research Article)
DOI: 10.30499/IJG.2021.268689.1314

Estimation of elastic moduli based on Pre-stack simultaneous inversion of an oil field in the Persian Gulf

Vahid Kameli Nia [1], Ali Misaghi[2*] and Yasser Basati[3]

[1] *Ms.c Student of Geophysics, Faculty of Earth Sciences, Kharazmi University, Tehran, Iran*
[2] *Assistant Professor of Geophysics, Faculty of Earth Sciences, Kharazmi University, Tehran, Iran*
[3] *Ms.c Graduate of Geophysics, Faculty of Earth Sciences, Kharazmi University, Tehran, Iran*

(Received: 20 december 2020, Accepted: 22 June 2021)

Abstract

Proper utilization of 3D seismic data in the upstream oil industry is one of the crucial steps in field developments. Many attributes are used to obtain models of facies distribution in a reservoir. Using prestack inversion methods on 3D seismic data and extracting prestack attributes such as elastic properties play very important roles in precise estimation of reservoir properties. The results of prestack seismic inversion in the oil reservoirs are investigated in this study. Simultaneous prestack inversion provides more details of acoustic impedance section rather than the poststack inversion. Moreover, the compressional acoustic impedance extracted from simultaneous inversion is more accurate than the one obtained from poststack inversion. In addition to the compressive acoustic impedance, shear impedance and density, the elastic parameters can be extracted from simultaneously prestack inversion. The purpose of this research is to transform the prestack inversion products into the geomechanical parameters including Young's modulus and Poisson's ratio. Young's modulus and Poisson's ratio have been used in geophysical algorithms to detect the well drilling trajectory and estimate the stress direction. These parameters can also be used in fluid detection studies.

Keywords: Elastic modulus, simultaneous prestack inversion, poststack inversion, acoustic impedance

[*] Corresponding author: ali.misaghi@gmail.com

1 Introduction

The only way that can definitely be mentioned to identify the lithology and to prove the presence of fluid in the reservoirs is to drill exploratory wells. But drilling the well will incur capital losses if it does not lead to cost-effective oil and gas extraction. Therefore, in order to reduce the risk of drywell, as well as to explore new hydrocarbon resources and increase productivity in the region, it is necessary to use advanced, quick and cost-effective methods. The studying of the reservoir behavior based on its physical properties can represent a pattern of rock balance (Soleimani, 2017). Human interventions such as drilling, production or injection disorder the balance of the rock structure. The results of these changes can be studied as rock mechanics (Zoback, 2010). Seismic geomechanical studies investigate the strain of rocks against the stresses on them and the factors affecting this interaction. In fact, geomechanics is the common intersection of rock mechanics, structural geology, and geophysics. One of the most important steps in characterizing the reservoir is to identify the relationship between the geomechanical and elastic properties of rocks (Rickman et al., 2008). Poisson's ratio (ν) and Young's modulus (E) obtained from inversion process can be used to determine areas with low clay content and high rigidity throughout the survey area. The main goal of seismic inversion is to calculate the P- and S-wave velocity, then the P- and S-impedance in order to characterize the reservoir in more detail in terms of the lithology, porosity and the type of the reservoir fluid (Xiang and Lubis, 2017). Ødegaard and Avseth (2003) suggested a method in which the cross plot of P- impedance versus V_P / V_S ratio can be used to determine the hydrocarbon content and mineral composition of the reservoir. Perez (2010) stated that the use of elastic physical parameters of rocks as well as Lamé parameters can geomechanically characterize a reservoir. Most of the geotechnical studies estimate the geomechanical behavior of fracturing survey based on Young's modulus and Poisson's ratio. Since it is difficult to measure density from surface seismic data, Sharma and Chopra (2012) used ρE and ν, which leads to volumetric 3D estimates of geomechanical behavior. The suggested approach integrates several parameters such as petrophysical data, well log analysis results and simultaneous seismic inversion outputs. This enables a more accurate description of the reservoir. Owing to the simultaneously extraction of acoustic impedance, density and V_P / V_S ratio for reservoir characterization with a proper accuracy (Ahmed, 2014), the above-mentioned studies used the simultaneous prestack inversion method. Kidambi and Kumar (2016) performed in-situ geomechanical analysis to create a one-dimensional mechanical earth model (MEM) for a vertical well drilled in carbonate gas reservoirs. In one-dimensional modeling, data representing static properties (such as petrophysical logs) is used to classify the earth model based on the geomechanical and static properties. This research contains well logs and 3D angle stacks of seismic data from studied area. The seismic data encloses 301 cross-lines and 561 inlines at different ranges of angle stacks, near (1°–10°), mid (10°–20°) and far (20°–29°). The normal bin size is 12.5×12.5 and the sampling interval is 2 ms. Check shots and well logs data were available in two wells.

2 Methodology

There are several methods for inversion of seismic data and achieving the earth model. Each method uses a specified algorithm for extraction of rock and fluid properties. Regardless of the details of each method, they can generally be divided into two types of prestack and post-stack methods. These methods use the

reflectivity of the boundary between layers to obtain effective elastic properties in each layer. In this study, simultaneous prestack inversion is used. This inversion algorithm produces initial models for density and P- and S-impedance, by assigning a set of traces in the same angular range and wavelets to each range (Sumanta et al., 2018). For each angle range, an appropriate wavelet must be calculated. Three wavelets were extracted for near, mid and far angles. Then, using well log, the optimal values for m, K_C, k and m_c are calculated (These parameters are regression coefficients of well cross plots and will be introduced later). In the case of simultaneous prestack inversion, it is initially assumed that the ratio of the S-wave velocity over the P-wave velocity in clastic rock layer should be constant. Based on this assumption, the following relation can be written (Hampson et al., 2005):

$$ln(Z_S) = ln(Z_P) + ln(V_S/V_P) \quad (1)$$

where Z_P is P-impedance and Z_s is S-impedance. Assuming a linear relationship between Z_P and Z_S:

$$ln(Z_S) = k\ ln(Z_P) + K_c + \Delta L_S \quad (2)$$

where k is the slope of the fitted line related to the logarithm of shear impedance versus the logarithm of acoustic impedance cross plot. K_C is the intercept of the mentioned cross plot and ΔL_S is the effect when the rock fluid is not water (Moghanloo et al., 2018).

The other assumption is that the Gardner equation for studying density derived from laboratory measurements is given by the following relationship (Gardner et al., 1974):

$$\rho = \alpha V_P^{\beta} \quad (3)$$

where ρ is the bulk density and α and β are constants obtained empirically. It can be shown that ρ is mathematically equivalent to the following equations:

$$ln(\rho) = \frac{(\beta)}{(\beta+1)} ln(Z_P) + \frac{ln(\alpha)}{(\beta+1)} \quad (4)$$

$$ln(\rho) = m\ ln(Z_P) + m_C + \Delta L_D \quad (5)$$

In Eq. (5), m is the slope of the fitted line related to the natural logarithm of density versus the natural logarithm of acoustic impedance cross plot and m_C is the intercept of the mentioned cross plot. ΔL_D is the effect when the rock fluid is not water (Moghanloo et al., 2018).

Aki-Richards equation (Aki and Richards, 2002) modified by Fatti et al. (1994) is given by:

$$R_{PP}(\theta) = C_1 R_P + C_2 R_S + C_3 R_D \quad (6)$$

The three reflectivity terms are given by:

$$R_P = \frac{1}{2}\left(\frac{\Delta V_P}{V_P} + \frac{\Delta \rho}{\rho}\right) = \frac{1}{2}\Delta\ ln(Z_P) \quad (7)$$

$$R_S = \frac{1}{2}\left(\frac{\Delta V_S}{V_S} + \frac{\Delta \rho}{\rho}\right) = \frac{1}{2}\Delta\ ln(Z_S) \quad (8)$$

$$R_D = \frac{\Delta \rho}{\rho} = \Delta\ ln\ \rho \quad (9)$$

From the zero offset that has occurred by combining the above equations, the trace angle can be extended as:

$$T(\theta) = \frac{1}{2}C_1 W(\theta) DL_P + \frac{1}{2}C_2 W(\theta) DL_S = \frac{1}{2}C_3 W(\theta) DL_D \quad (10)$$

where $W(\theta)$ is wavelet at angle θ, $L_P = ln(Z_P)$ and $L_S = ln(Z_S)$. Estimation of initial model requires determination of coefficients and parameters (m_c, m, k_c, k), which are determined using acoustic and density logs. An initial estimate is made for the following equation extracted from Eq. (10) and is written as matrix (Hampson et al., 2005):

$$[L_P \quad \Delta L_S \quad \Delta L_P]^T = [log(Z_{P0}) \quad 0 \quad 0]^T \quad (11)$$

Z_{P0} is the initial model of impedance. By solving this equation, the final values of Z_P, Z_S and density are calculated according to the following equations (Hampson et al., 2005):

$$Z_P = exp\ (L_P) \quad (12)$$

$$Z_S = exp\ (kL_P + k_c + \Delta L_S) \quad (13)$$

$$\rho = exp\ (mL_P + m_c + \Delta L_D). \quad (14)$$

3 Well tie and wavelet extraction

Used to generate the synthetic seismograms, the wavelet is a key element in inversion process and well-to-seismic correlation. In prestack seismic data, it is known that the seismic data will loss high frequency energy from near to far offset (Hampson et al., 2005). Therefore, the amplitude, frequency and representation of none of the common depth point (CDP) gathers will be the same. This study extracts statistical wavelets and compares them for determining which wavelets can lead to more accurate inversion results (Fig. 1). Reflection coefficients are obtained from acoustic and density logs. By convolution of reflection coefficients and extracted wavelet from seismic data, synthetic traces are obtained. If the extracted wavelet is suitable, the synthetic traces will have good correlation with the seismic data. To achieve this goal, the seismic data were divided into three sets of angle gathers and the wavelets were statistically extracted for each angle set.

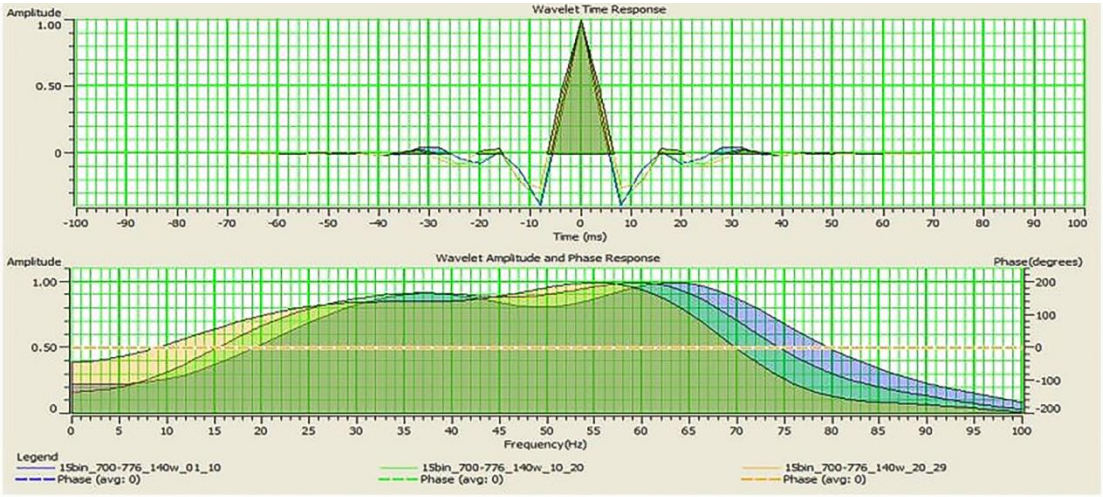

Fig 1. Extraction of statistical group wavelets for near, mid and far angle gathers.

4 Generate low frequency model

Building the low frequency model is one of the important steps that must be considered in the seismic inversion processing because the volumes obtained from inversion without the low frequency model will give only the approximate properties of the rock. Furthermore, using initial model helps to make high coefficient of correlation. Acoustic impedances obtained in the inversion step and low frequency model are used in the evaluation of reservoir properties (Sumanta et al., 2018). The required data to build the initial model are the P- and S-velocity and density obtained from the petrophysical well logs. Seismic horizons are also used to define different reservoir and non-reservoir levels (Fig. 2).

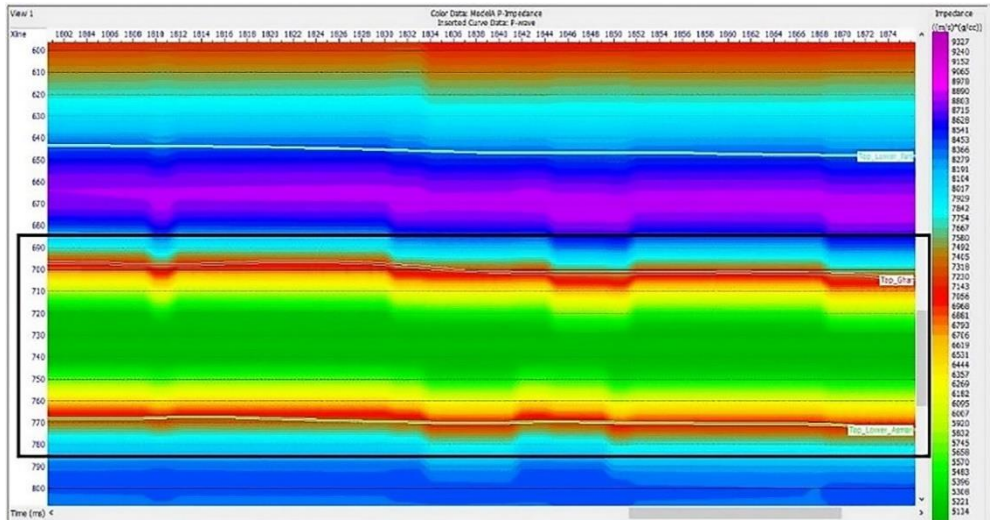

(a)

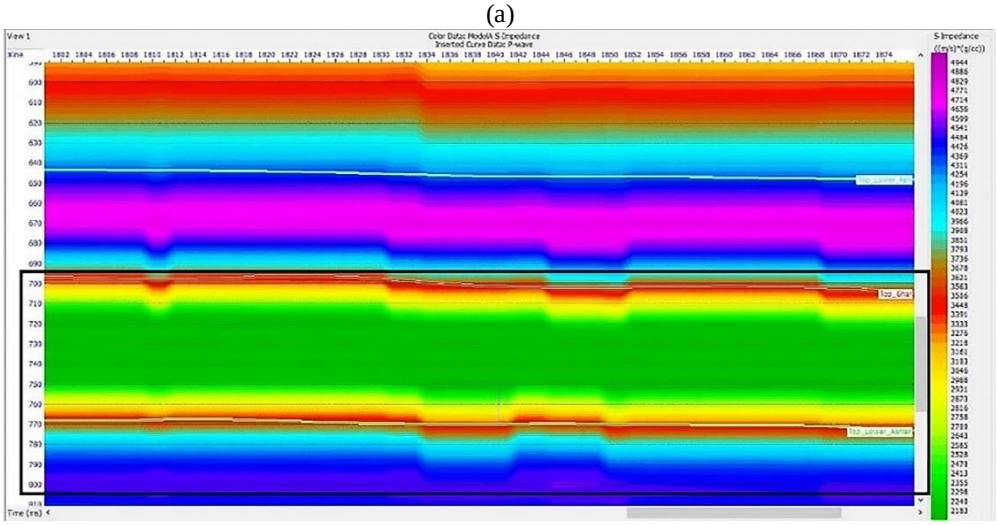

(b)

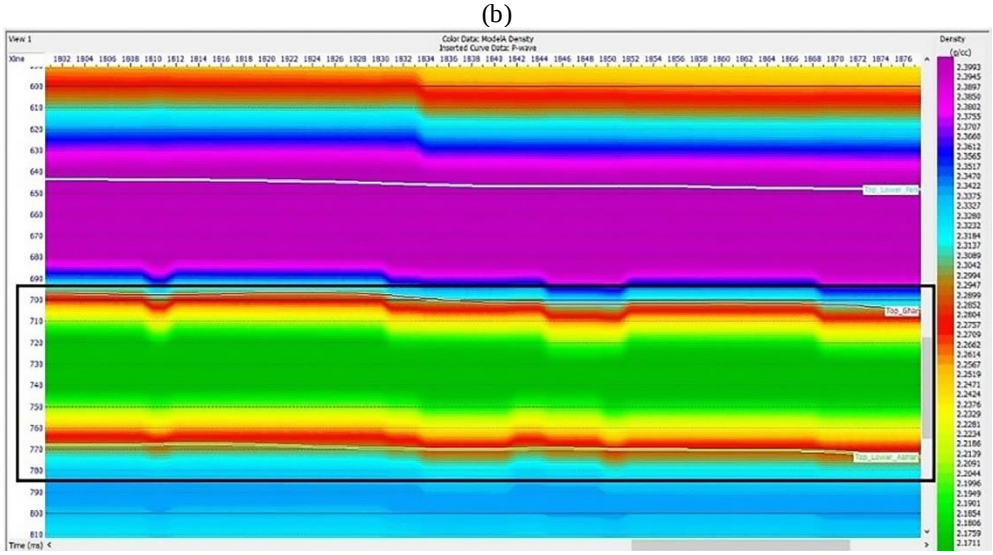

(c)

Fig 2. Initial model building. (a) P-impedance (b) S-impedance (c) density.

It is assumed that the linear relationship between the variables (Z_P, Z_S, density) occurs in the absence of hydrocarbons. Deviations away from a linear fit indicate presence of hydrocarbon (Fig. 3).

Table 1. Optimal regression coefficients for well cross plots.

Regression coef.	k	K_C	m	m_c
Value	1.2	-2.572	0.326	-2.07

5 Inversion analysis

Simultaneous inversion processing was applied to the whole seismic volume. The output parameters of inversion in the wells were compressional acoustic impedance, shear acoustic impedance and density. In this step, the output of simultaneous inversion will be the sections of these three inverted volumes shown in Figs. 4, 5 and 6. Fig. 4 is a cross-section of P-impedance (Z_P) in which the color scale shows the amount of change in the parameter. The higher Z_P value indicates the higher incompressibility. The presence of anhydrite cap rock was observed at the top of the reservoir, which has the highest value of P-impedance. As seen in Fig. 4, in the Ghar sandstone reservoir, the amount of P-impedance is less than the upper and lower layers. A layer with a high impedance difference can also be seen in the upper Asmari Formation, which could be related to the dolomitic layer containing gas. Notable reduction in P-impedance is due to the differences in lithology, high porosity and especially the presence of hydrocarbons. In the S-impedance section (Fig. 5), the presence of high impedance areas in the reservoir relative to the general trend of the reservoir indicates the presence of layers with different lithological features (clay thin layers) than the main reservoir rock (sandstone). Fig. 6 shows the inverted density section. In the Ghar reservoir (black rectangle) and the gas bearing layer (black ellipse), this parameter is significantly reduced as compared to the adjacent layers.

Fig. 7 demonstrates the well logs of one of the wells. As shown, density and S- and P-wave velocities decrease in interested area. To validate the prestack inversion outputs, well logs were used.

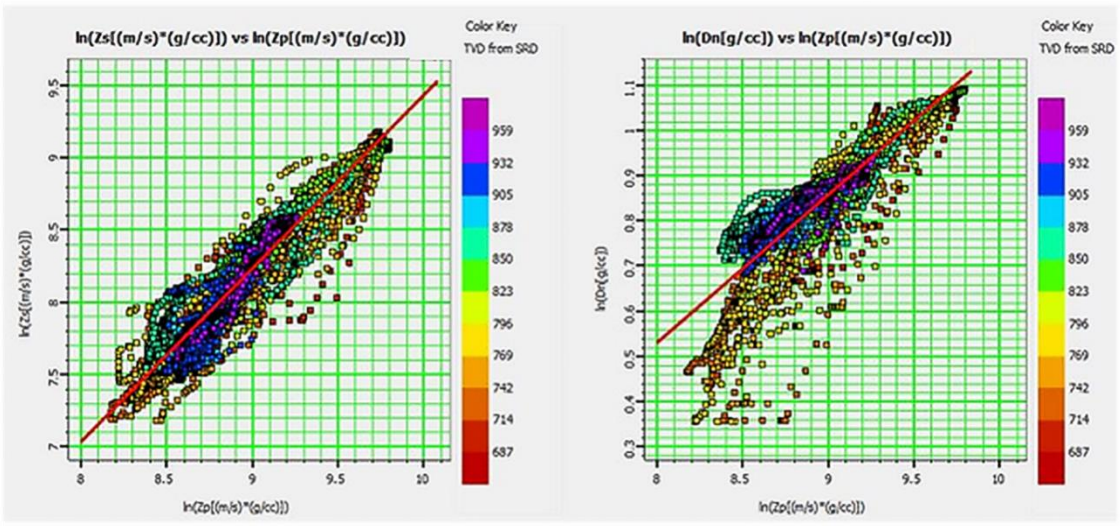

(a) (b)

Fig 3. Determining m_c, m, k and K_c values using (a) cross plot of S-impedance logarithm versus P-impedance logarithm obtained from well log data, and (b) cross plot of density logarithm versus P-impedance logarithm.

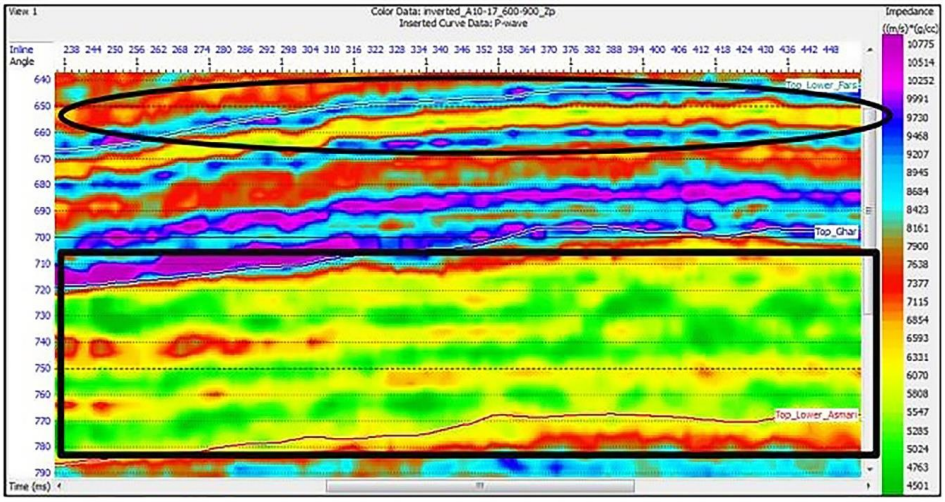

Fig 4. P-impedance section obtained from inversion in the Ghar reservoir. Z_P parameter is significantly reduced compared to the overlaying and underlying layers. Moreover, in the upper Asmari Formation section, there is a layer with high impedance, which can be related to the dolomitic layers of this zone.

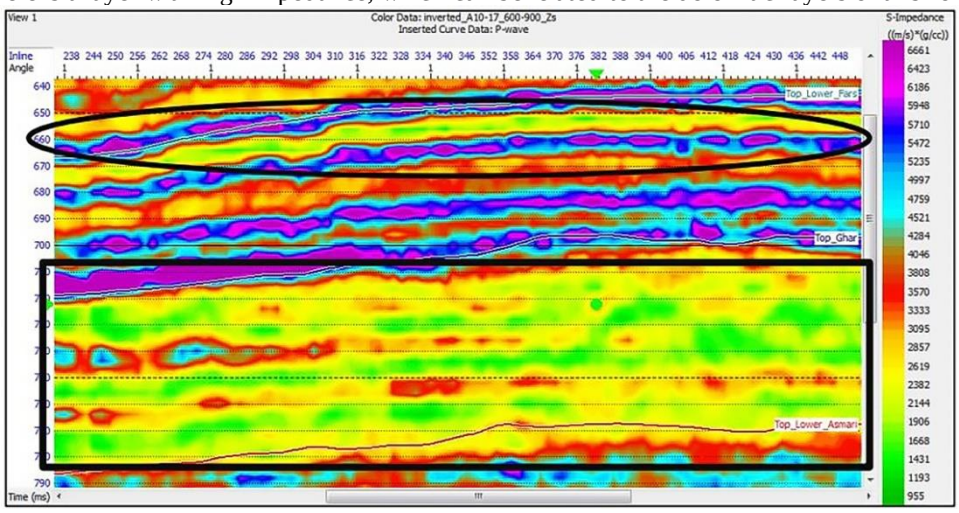

Fig 5. S-impedance section obtained from inversion. In the scope of Ghar reservoir and gas bearing layers in the Asmari Formation, this parameter is reduced significantly than the surrounding layers.

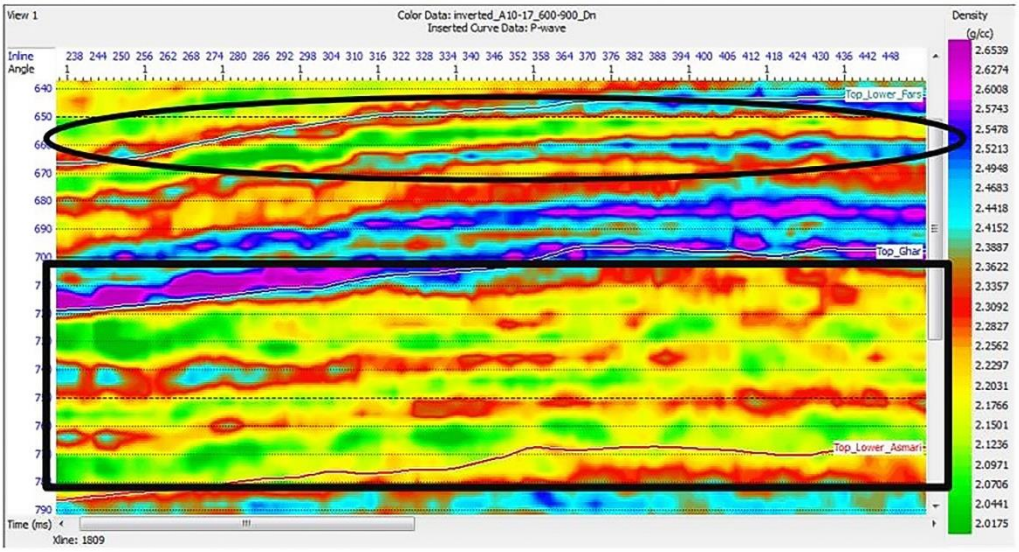

Fig 6. Inverted density section. In the Ghar reservoir (black rectangle) and the gas bearing layer (black ellipse), this parameter is significantly reduced as compared to the adjacent layers.

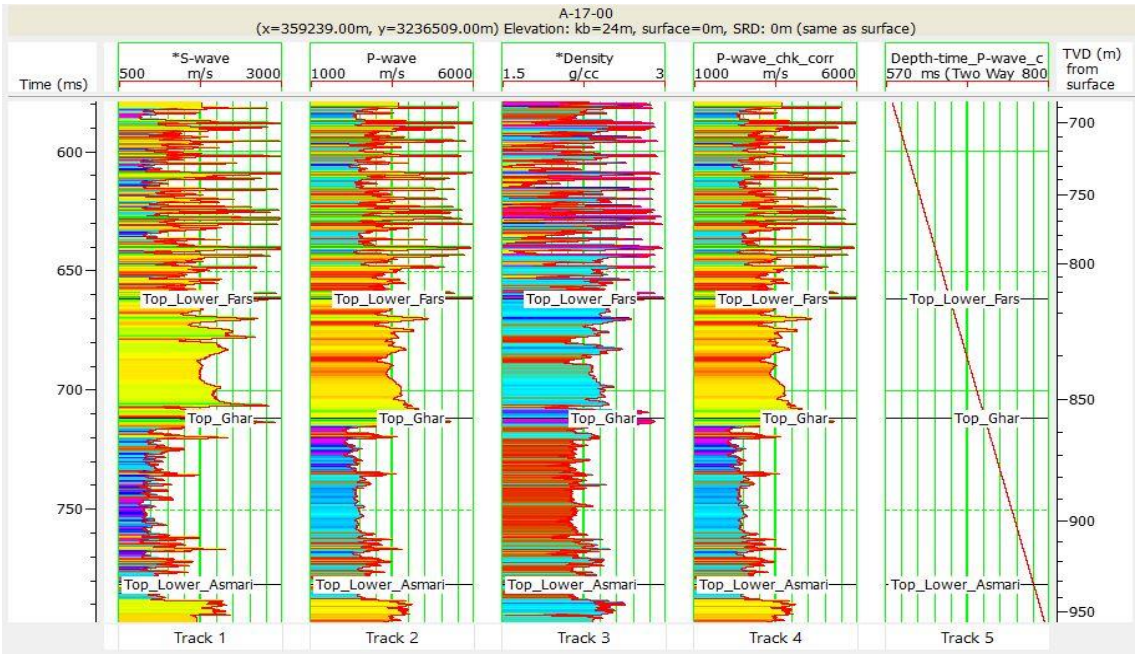

Fig 7. S-wave velocity, P-wave velocity and density logs and applied check shot on A-17 well in the area.

6 Elastic parameters analysis

Young's modulus, E, is defined as the ratio of the axial stress to the axial strain in uniaxial compression. Poisson's ratio, *v*, is defined as the negative of the ratio of the lateral strain to the axial strain in uniaxial compression (Perez, 2014). After inverting the entire scope of the seismic data and obtaining the output parameters, the elastic parameters are calculated. Density and shear wave velocities can be calculated by dividing the impedance sections over the density. Using the input parameters (velocity and density), the desired elastic parameters can be calculated. Fig. 8 shows the elastic parameters. In the reservoirs zone, elastic parameters were used for fluid identification. In section (a) of the Young's modulus, values in the range of 35 GPa in the cap rock have been reduced to the range of 5 GPa in the reservoir. In Fig. 9, the Poisson's ratio has increased from 0.23 in the area to 0.43 in the cap rock. Furthermore, in both sections, a gas bearing dolomitic layer can be identified in the upper Asmari Formation. Due to the presence of inter-bedding shale layers (with lower porosity and permeability than sandstone containing hydrocarbons) in some parts of the reservoir, the Young's modulus increases by 13 GPa compared to sandstone. This trend is also observed for the Poisson's ratio in clay layers and decreases by 0.2 compared to sandstone, which is due to a significant reduction in porosity and fluid substitution in these layers.

7 Pore pressure

The pore pressure is the pressure exerted by the fluid in the rock and withstands the overburden stress (Eaton, 1975). There are several methods of predicting pore pressure based on logging and seismic data. Eaton's equation (15) uses the wave travel time factor and formation wave velocity to measure pore pressure:

$$P_P = S - (S - P_{hyd})\left(\frac{\Delta T_n}{\Delta T_{log}}\right)^3 \qquad (15)$$

where P_P is pore pressure, S is overburden stress, P_{hyd} is hydrostatic pressure, ΔT_n is the normal trend attenuation and ΔT_{log} is the attenuation measured by well log. Using well log data and the elastic parameters extracted from inversion, the pore pressure of one of the wells was cal-

culated. Based on the shallow depth of the Ghar reservoir, the pore pressure does well follow the hydrostatic pressure. The normal trend attenuation for the dolomitic-shale part of the Ghar horizon is assumed to be 90 microseconds. The obtained values for the pore pressure are 7.6 to 7.7 MPa and its gradient is 0.45 to 0.46 psi. The pore pressure gradient is almost equal to the hydrostatic pressure gradient (0.44 psi).

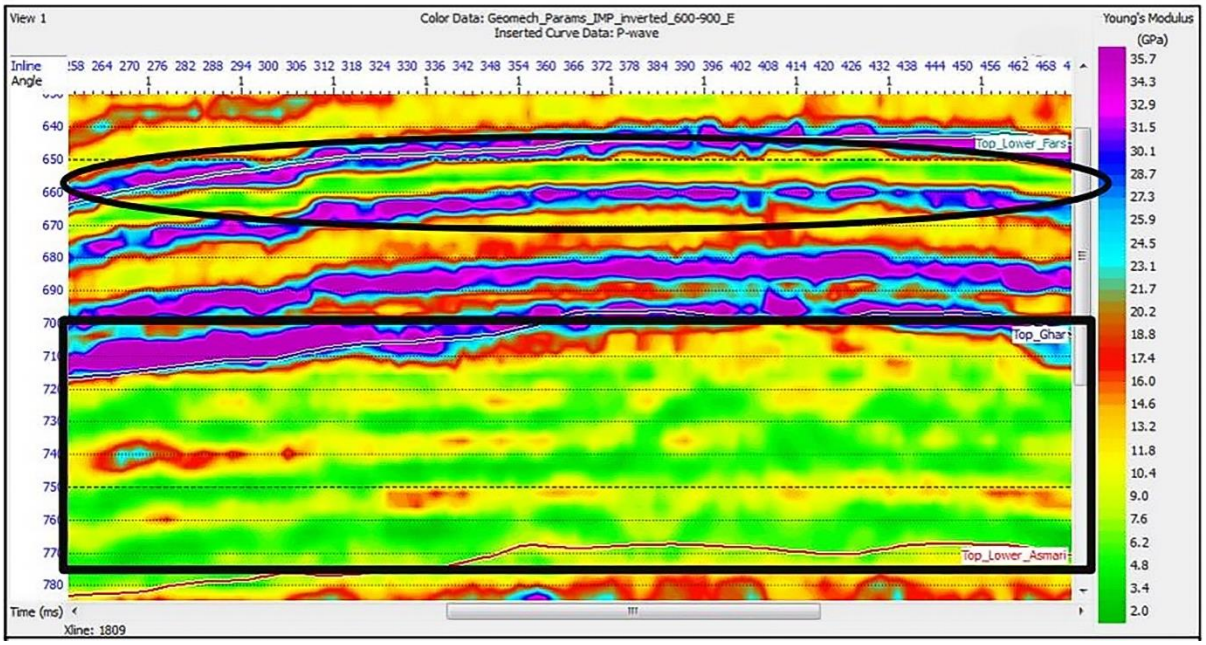

Fig 8. Young's modulus section. This elastic parameter has been extracted from inversion. In the area of the reservoir (rectangular) and the gas-bearing layer (ellipse), the amount of Young's modulus has decreased significantly compared to the anhydrite-shale cap rock.

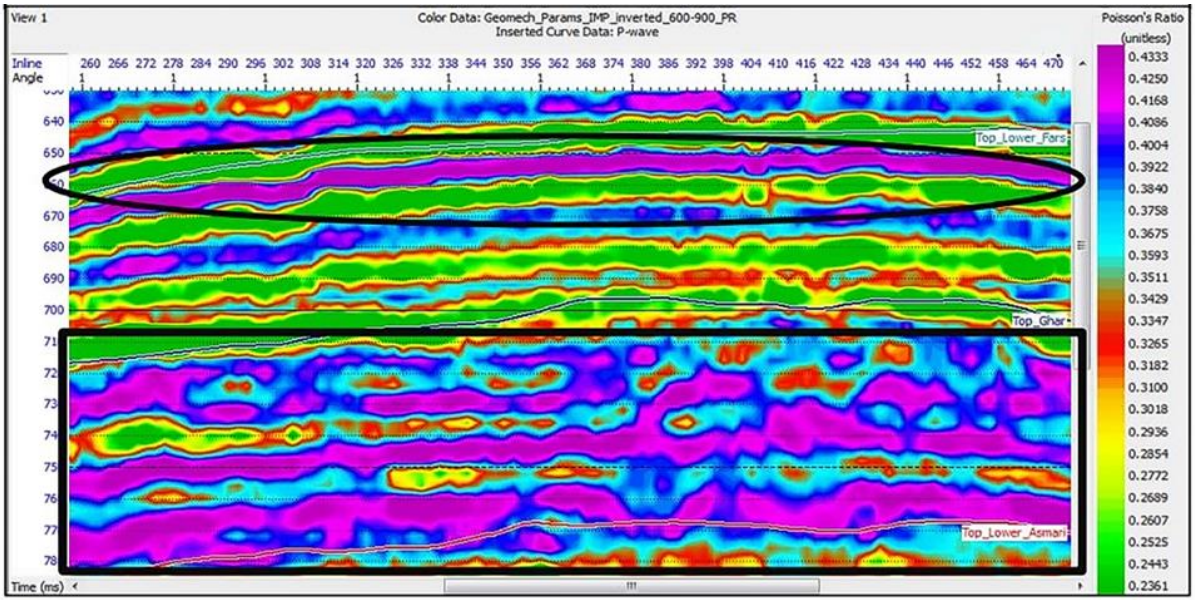

Fig 9. Poisson's ratio section. This elastic parameter has been extracted from inversion. The Poisson's ratio has increased significantly in the area.

8 Mechanical Earth Model (MEM)

The MEM provides the mechanical properties of the reservoir and sedimentary basin. In addition to the numerical distribution of reservoir rock properties (such as porosity and density) and fracture system, this model also expresses pore pressure, stress and mechanical properties of the reservoir (Plumb et al., 2000). Geomechanical model contains the depth sections of elastic parameters, rock strength and the earth stresses. In the one-dimensional geomechanical model, the changes in the parameters mentioned along the well and the changes in the stratigraphic columns are determined. The main component of the geomechanical model is information about the in-situ stress situation of the reservoir. Figs. 10 and 11 represent the one-dimensional geomechanical parameter model, calculated in the A-17 well under reservoir conditions.

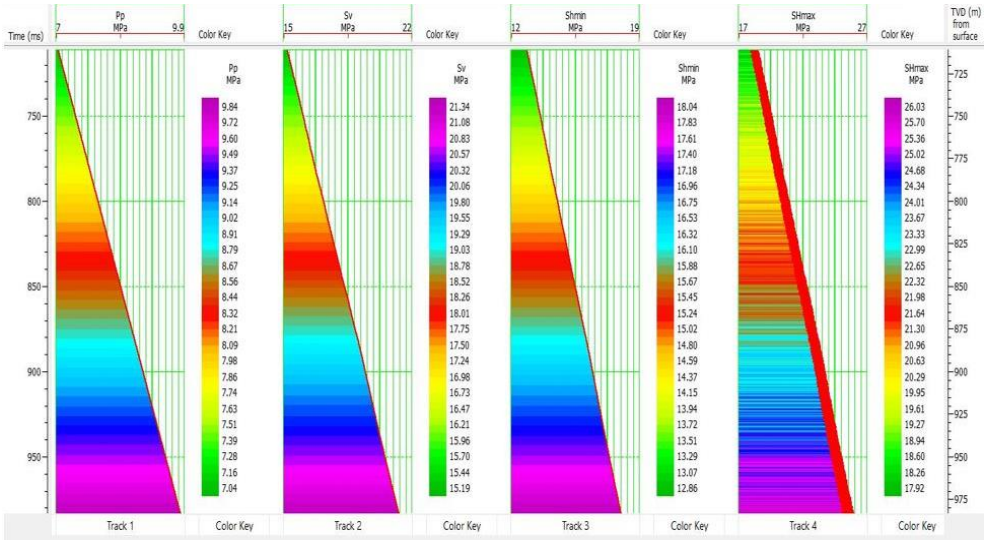

Fig10. One-dimensional model of geomechanical parameters in well A-17 under reservoir conditions. Left to right: pore pressure, overburden stress, minimum horizontal stress and maximum horizontal stress.

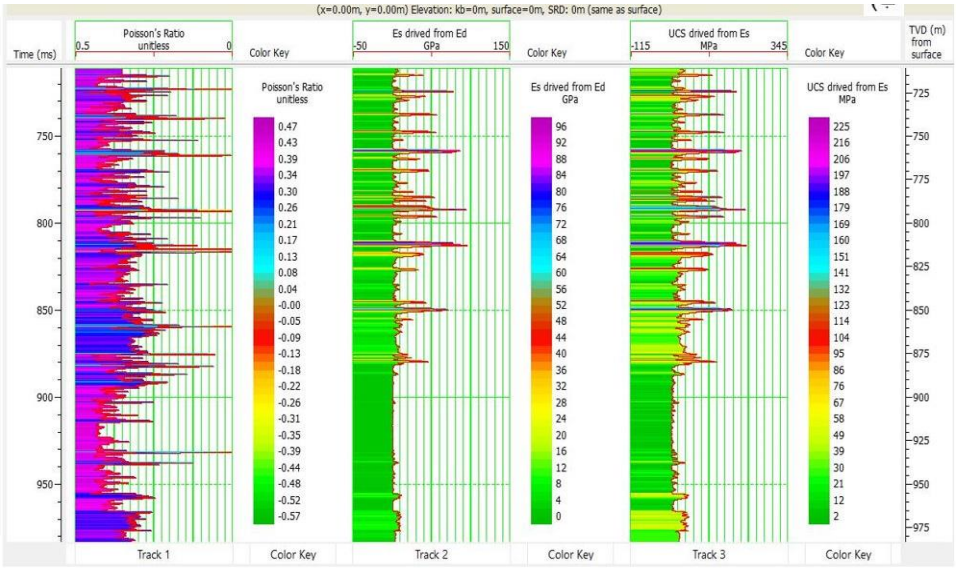

Fig 11. One-dimensional model of geomechanical parameters in well A-17 under reservoir conditions. Poisson's ratio and static Young's modulus (Es) derived from dynamic Young's modulus (Ed). *Uniaxial* compressive *strength (UCS) derived from* static Young's modulus.

Conclusion

In this study, Young's modulus and Poisson's ratio were estimated in an oil field in the Persian Gulf based on the simultaneous prestack inversion approach. Some other parameters such as density, compressional and shear wave impedance were estimated successfully. The results of this study show that the Young's modulus decreases in the zone of Ghar reservoir. Implementation of inversion process produced three models of compressive impedance, shear impedance and density as outputs. Using inversion outputs, the elastic parameters (Young's modulus and Poisson's ratio) in the field range were calculated. The parameters of P-impedance, S-impedance and density in the area of the Ghar hydrocarbon reservoir as well as the gas bearing layer in the upper Asmari Formation are significantly reduced. The Young's modulus parameter decreases in the area of Ghar hydrocarbon reservoir as well as the gas bearing layer in the upper Asmari Formation. However, the Poisson's ratio increases in the Ghar reservoir as well as the gas bearing reservoir in the upper Asmari Formation. In addition, the mentioned moduli were utilized in geomechanical analysis to evaluate the strength of the rock to maintain fracture and its breaking capacity under stress conditions. Therefore, some parts of the reservoir that have high Young's modulus are prone to hydraulic fracturing operations to increase productivity.

Reference

Ahmed, Z., 2014, Pre-stack simultaneous inversion of 3D seismic data for velocity attributes to delineate channel sand reservoir: International Journal of Emerging Technology and Advanced Engineering, **4**, 69–78.

Aki, K., and Richards, P. G, 2002, Quantitative seismology.

Eaton, B. A., 1975, The equation for geopressure prediction from well logs: in Fall meeting of the Society of Petroleum Engineers of AIME, Society of Petroleum Engineers.

Fatti, J. L., Smith, G. C., Vail, P. J., Strauss, P. J., and Levitt, P. R., 1994, Detection of gas in sandstone reservoirs using AVO analysis: a 3D seismic case history using the geostack technique: Geophysics, **59** 1362–1376.

Gardner, G. H. F., Gardner, L. W., and Gregory, A. R., 1974, Formation velocity and density—The diagnostic basics for stratigraphic traps: Geophysics, **39**(6), 770-780.

Hampson, D. P., Russell, B. H., and Bankhead, B., 2005, Simultaneous inversion of prestack seismic data: SEG Technical Program Expanded Abstracts 2005, Society of Exploration Geophysicists, 1633-1637.

Kidambi, T., & Kumar, G. S., 2016, Mechanical earth modeling for a vertical well drilled in a naturally fractured tight carbonate gas reservoir in the Persian Gulf. Journal of Petroleum Science and Engineering, *141*, 38-51.

Moghanloo, H. G., Riahi, M. A., and Bagheri, M., 2018, Application of simultaneous prestack inversion in reservoir facies identification: J. Geophys. En., **15**(4), 1376–1388, doi 10.1088/1742-2140/aab249.

Perez, R., 2010, Application of LMR inversion and clustering analysis in the Barnett Shale: 80th Annual International Meeting, SEG, Expanded Abstracts, 2236–2239.

Perez, R., 2014, Brittleness estimation from seismic measurements in unconventional reservoirs: Application to the Barnett shale, Proquest, 2014.

Plumb, R., Edwards, S., Pidcock, G., Lee, D., and Stacey, B., 2000, The mechanical earth model concept and its application to high-risk well construction projects: IADC/SPE Drilling Conference, Society of Petroleum Engineers.

Rickman, R., Mullen, M. J., Petre, J. E., Grieser, W. V., and Kundert, D., 2008,

A practical use of shale petrophysics for stimulation design optimization: All shale plays are not clones of the Barnett Shale: SPE Annual Technical Conference and Exhibition, Society of Petroleum Engineers.

Sharma, R. K., and Chopra, S., 2012, New attribute for determination of lithology and brittleness: 82nd Annual International Meeting, SEG, Expanded Abstracts, doi 10.1190/segam2012-1389.1.

Soleimani, M., 2017, Naturally fractured hydrocarbon reservoir simulation by elastic fracture modeling: Petroleum Science, **14**(2), 286-301.

Sumanta, R., Rosid, M. S., and Adrianto, R. D., 2018, Characterization sandstones reservoir using simultaneous inversion method in Sungai Lilin field: AIP Conference Proceedings, **2023**(1), 020255, AIP Publishing LLC.

Xiang, L. M., and Lubis, L. A., 2017, Application of simultaneous inversion characterizing reservoir properties in X field, Sabah Basin: IOP Conference Series: Earth and Environmental Science, **88**(1), 012022, IOP Publishing.

Zoback, M. D., 2010, Reservoir Geomechanics: Cambridge University Press.

Ødegaard, E. R. I. K., and Avseth, P., 2003, Interpretation of elastic inversion results using rock physics templates: 65th EAGE Conference and Exhibition, cp-6, European Association of Geoscientists and Engineers.